

# Local density of states and scattering rates across the many-body localization transition

Atanu Jana<sup>1</sup>, V. Ravi Chandra<sup>1</sup>, Arti Garg<sup>2</sup>

<sup>1</sup> *School of Physical Sciences, National Institute of Science Education and Research Bhubaneswar, HBNI, Jatni, Odisha 752050, India and*

<sup>2</sup> *Theory Division, Saha Institute of Nuclear Physics, 1/AF Bidhannagar, Kolkata 700 064, India*

Characterizing the many-body localization (MBL) transition in strongly disordered and interacting quantum systems is an important issue in the field of condensed matter physics. We explore the single particle Green's functions, the corresponding local density of states and the self energy for a disordered interacting system using exact diagonalization in the infinite temperature limit of the MBL system. We provide strong evidence that the typical value of the scattering rate obtained from the imaginary part of the self energy and the local density of states can be used to track the delocalization to MBL transition. In the delocalized phase, the typical value of the local density of states and the scattering rate is of the order of the corresponding average values while in the MBL phase, the typical value for both the quantities becomes vanishingly small. The probability distribution function of the local density of states and the scattering rates are broad log-normal distributions in the delocalized phase while the distributions become very narrow and sharply peaked close to zero in the MBL phase. We also study the eigenstate Green's function to obtain the scattering rates and the local density of states for all the many-body eigenstates and demonstrate that both, the energy resolved typical scattering rates and the typical local density of states, carry signatures of the many-body mobility edges.

The physics of Anderson localization [1] in non-interacting disordered quantum systems has been a cornerstone of condensed matter theory. Turning on interactions in these disordered systems results in many-body localized (MBL) phase where the system lacks transport [2–6] up to a finite temperature. In the MBL phase, the system ceases to act as its own bath due to its non-ergodic nature and hence an isolated quantum system in the MBL phase can not thermalize [5, 6]. Thus, the lack of ergodicity which is generally identified using the statistics of level spacing ratio [4] and the violation of eigenstate thermalization hypothesis [7–9], are among the crucial characteristics of the MBL phase. The non-ergodic nature of the MBL phase is also reflected in the quantum quench studies where the system in the MBL phase shows a strong memory of the initial state which has made the time evolution of the density imbalance [4] a popular tool to analyze the MBL phase both theoretically [10–15] and experimentally [16]. The MBL phase has also been shown to have local integrals of motion [17] which are exponentially localized operators which commute with each other and the Hamiltonian.

The delocalization to localization transition is also tracked using the statistics of eigenfunctions [4, 18–21], scaling of subsystem entanglement entropy [4, 22–28] and extremal statistics of entanglement eigenvalues, as recently proposed [29]. Since the MBL transition is a dynamical transition that involves many higher excited states, all the analysis of eigenfunction statistics or the entanglement entropy is done for the entire many-body spectrum and not only for the ground state. Dynamical quantities like the return probability, which gives the

probability with which a quantum particle comes back to its initial position at a later time [14, 28, 30–33], time dependent density-density correlation functions [11, 34–37] and low-frequency conductivity [11, 32, 38–40] calculated in the infinite temperature limit have also been useful to identify the delocalized and the MBL phase.

In this work we explore the single particle Green's function in real space, calculated for the many-body eigenstates in middle of the spectrum or in the infinite temperature limit. We demonstrate that the delocalization to MBL transition can be tracked using the typical value of the local density of states and the single particle scattering rates. Though the local density of states (LDOS) has been extensively used to analyze the non-interacting Anderson localization [41–49], it has not been explored as much in the context of MBL. Recently, there have been works on evaluation of the propagator in the Fock space by mapping the many-body interacting Hamiltonian of the MBL problem to an effective non-interacting Anderson model [50, 51]. Here, we focus on the single-particle Green's function in real space and show that the typical value of the LDOS is finite in the delocalized phase, being of the order of its average value while in the MBL phase the typical value vanishes though the average value is still non-zero. The probability distribution of the LDOS in the delocalized phase looks very close to being a broad log-normal distribution while it becomes a very narrow distribution in the MBL phase. We also calculate the infinite temperature self-energy by comparing the Green's function of the interacting and the non-interacting disordered system. Our numerical results show clear evidence of how the distribution of the scattering rate, which is

obtained from the imaginary part of the self energy, can be used to track the delocalization to MBL transition. In complete analogy with the LDOS, the typical scattering rate is finite being of the order of its average value in the delocalized phase while in the MBL phase the typical scattering rate is vanishingly small while the average scattering rate is still finite. The transition point obtained from this analysis is consistent with the one obtained from the level spacing ratio. We further analyzed the Green's functions for all the many-body eigenstates which carry signatures of the many-body mobility edges and are consistent with the energy resolved picture obtained from a more conventional quantity like level spacing ratio.

There have been earlier works on the LDOS in the ground state of disordered interacting systems (with spinful fermions) using various versions of dynamical mean field theory [52] as well as other approaches [53] for  $d \geq 2$  Anderson-Hubbard model. Most of these studies showed a transition from single particle Anderson localization to Mott insulator via an intermediate metallic phase as the interactions strength is increased for a fixed disorder strength. In this work, instead of focusing on a detailed analysis of the ground state, we analyze the single particle Green's functions in the infinite temperature limit of a finite size system using exact diagonalisation. For a one-dimensional model of spinless fermions, treating interactions and disorder exactly, we calculate the eigenstate Green's function and the self energy for all the many-body eigenstates. Typical values of the LDOS and the scattering rates calculated for the many-body eigenstates in the middle of the spectrum carry clear signatures of the MBL transition. Since many-body states in the middle of the spectrum get localized in the end as the disorder strength increases, our analysis attempts to capture salient features of the MBL transition which would be missed if one restricts the analysis only to the ground state.

To be specific, we study the model often used for the study of the MBL transition, namely, the one-dimensional model of spinless fermions in the presence of random disorder and nearest neighbor repulsion. The Hamiltonian of the model studied is

$$H = -t \sum_i [c_i^\dagger c_{i+1} + h.c.] + \sum_i \epsilon_i n_i + V \sum_i n_i n_{i+1} \quad (1)$$

with periodic boundary conditions. Here, the onsite energy  $\epsilon_i \in [-W/t, W/t]$  is uniformly distributed, with  $W$  as the disorder strength,  $V$  is fixed to  $t (= 1)$  in the entire analysis and the system is half-filled. We solve the model using exact diagonalization, for several system sizes from  $L = 12$  to  $L = 20$ , to obtain the full set of energy eigenvalues  $E_n$  (for all system sizes) and eigenfunctions  $|\Psi_n\rangle$  (till  $L = 18$ ). The model in Eqn (1), which can also be mapped to a model of interacting spin-1/2 particles by Jordan-Wigner transformation [54], has been extensively

studied in context of MBL and a transition from the delocalized phase to the MBL phase is seen as the disorder strength  $W$  increases [25]. However, to the best of our knowledge, the analysis of the single particle LDOS and the self energy for this model in the infinite temperature limit to look for signatures of MBL has not been attempted before and this is the main focus of our work.

The Green's function in the  $n$ th eigenstate is defined as  $G_n(i, j, t) = -i\Theta(t)\langle\Psi_n|\{c_i(t), c_j^\dagger(0)\}|\Psi_n\rangle$  where  $i, j$  are lattice site indices. In the Lehmann representation, one can write the Fourier transform of  $G_n(i, i, t)$  as

$$G_n(i, i, \omega) = \sum_m \frac{|\langle\Psi_m|c_i^\dagger|\Psi_n\rangle|^2}{\omega + i\eta - E_m + E_n} + \frac{|\langle\Psi_m|c_i|\Psi_n\rangle|^2}{\omega + i\eta + E_m - E_n} \quad (2)$$

Here if  $|\Psi_n\rangle$  is the  $n$ th eigenstate of the Hamiltonian in Eqn. (1) for  $N_e$  particles in the chain, states  $|\Psi_m\rangle$  used in the first term of the Green's function expression in Eqn. (2) are obtained from diagonalization of  $N_e + 1$  particle system while the states  $|\Psi_m\rangle$  used in the second term of Eqn. (2) has been obtained from diagonalization of  $N_e - 1$  particle system.  $\eta$  is a positive infinitesimal and is set in our simulations to decide a finite broadening such that sufficient number of eigenstates fall in a bin of width  $\eta$ .

In this work, we will mainly focus on the Green's function calculated for eigenstates with eigenvalues  $E_n$  in the middle of the many-body spectrum to study the MBL transition. This is because many-body density of states of Eqn. (1) is sharply peaked in the middle of the spectrum for sufficiently large system, and hence an infinite temperature limit, which basically gives the average over the entire spectrum, will have dominant contribution from the many-body states in the middle of the spectrum. At the end, we also present results obtained by averaging over the entire many body eigen-spectrum, which gives an exact infinite temperature limit of the Green's function and the scattering rates. The local density of states  $\rho_n(i, \omega)$  and the self energy  $\Sigma_n(\omega)$  matrix obtained from the  $n$ -th eigenstate is given by:

$$\rho_n(i, \omega) = \left(-\frac{1}{\pi}\right) \text{Im} [G_n(i, i, \omega)]$$

$$\Sigma_n(\omega) \equiv \mathbf{G}_0^{-1}(\omega) - \mathbf{G}_n^{-1}(\omega)$$

Here  $\mathbf{G}_0(\omega)$  is the non-interacting Green's function matrix of the disordered system in Eqn (1). The scattering rate is identified as  $\Gamma_n(i, \omega) = -\text{Im} [\Sigma_n(i, i, \omega)]$ . The value of the infinitesimal  $\eta$  has been fixed to be  $10^{-2}$  for all the calculations. Furthermore, we compare the behavior of a commonly used diagnostic of the transition, namely the statistical behavior of level spacing ratios with the disorder averaged local density of states and the scattering rates obtained from the Green's functions

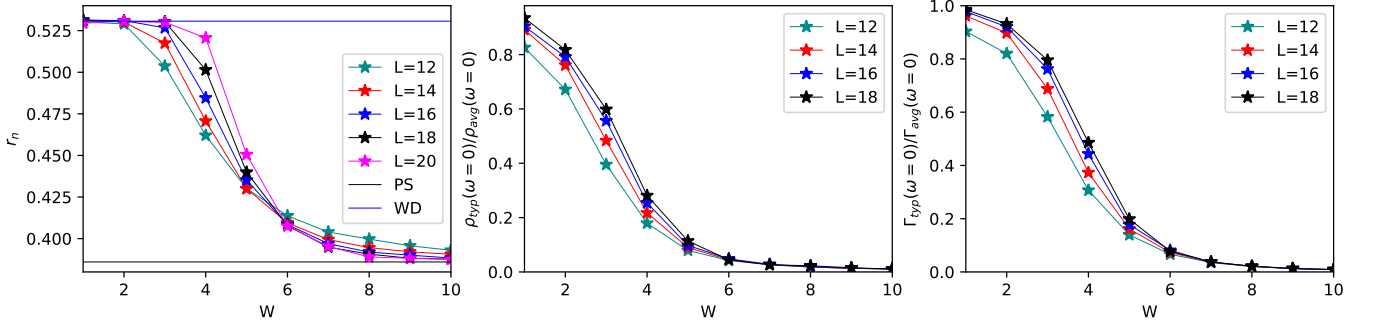


FIG. 1: First panel: the level spacing ratio for the mid spectrum eigenstates as a function of disorder strength  $W$  for various system sizes. Delocalization to MBL transition occurs at  $W \sim 6.0t$ . Second panel: the ratio of the typical to average local DOS  $\rho_{typ}(\omega=0)/\rho_{avg}(\omega=0)$ , calculated for the mid spectrum eigenstates at  $\omega=0$ , as a function of the disorder strength. The ratio is of order one for  $W \ll W_c$  and increases with  $L$ . For  $W > W_c$ , the ratio is vanishingly small and does not show any system size dependence. Similar trend is seen in the ratio of typical to average value of the scattering rate  $\Gamma_{typ}(\omega=0)/\Gamma_{avg}(\omega=0)$ , again calculated for the mid spectrum states. All quantities are computed for a rescaled energy bin  $E \in [0.495, 0.505]$

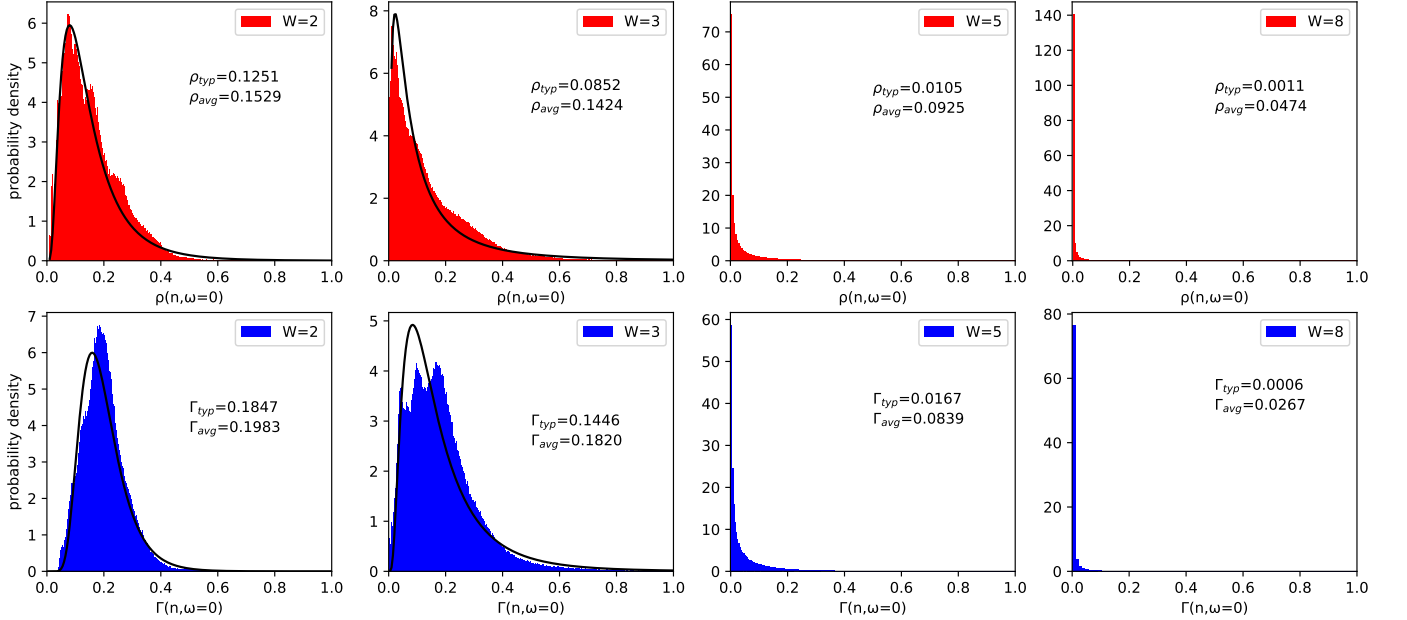


FIG. 2: Probability distribution function of the LDOS and the scattering rate at  $\omega=0$  for disorder strengths  $W=2, 3, 5, 8$  and  $L=18$ . These probability densities have been calculated in the middle of the spectrum for a rescaled energy bin  $E \in [0.495, 0.505]$ .

defined above. The level spacing ratios  $r_n$  are defined in the usual way  $r_n = \frac{\min(\delta_n, \delta_{n+1})}{\max(\delta_n, \delta_{n+1})}$ , where,  $\delta_n = E_{n+1} - E_n$ .

We compute the disorder averaged values of all the quantities defined above. The energy eigenvalues of each disorder realization are rescaled between  $[0, 1]$  and averages over disorder realizations are carried out for the same rescaled energy bin. For level spacing ratios we use averaging over 15000, 10000, 4000, 500 and 50 real-

izations of disorder for  $L=12, 14, 16, 18, 20$  respectively. For evaluation of typical values for the middle of the band we use 8000, 1000, 500 and 50 disorder realizations for  $L=12, 14, 16$  and 18 respectively. The typical values for LDOS and scattering rates are obtained by calculating the geometric average over all the lattice sites and independent disorder realizations, e.g. the typical value of the LDOS for the  $n$ -th eigenstate is given by,

$\rho_{typ}(n, \omega) = [\prod_{C_\alpha} \prod_{i=1}^L \rho_i(n, \omega)]^{1/CL}$ , where  $C$  is the number of independent disorder configurations and  $C_\alpha$  denotes a particular configuration. The definition for the typical scattering rate  $\Gamma_{typ}(n, \omega)$  is completely analogous. For calculations in the middle of the spectrum, we use a small bin  $E = 0.5 \pm 0.005$  centered around the rescaled energy  $E = 0.5$  and the typical values for that bin are evaluated using a geometric average over all the eigenstates within this bin before doing geometric averaging over lattice sites and disorder realizations. For the analysis of LDOS and scattering rates over the full band we use a similar method and divide the whole range  $E = [0, 1]$  into small bins and evaluate the typical values for each bin.

Fig. 1 depicts a comparison of these quantities as a function of the disorder strength in the middle of the many-body energy spectrum. The transition from the ergodic to non-ergodic behavior is clearly seen in the level spacing ratio  $r$  as the transition from Wigner-Dysonian (WD) to Poissonian statistics (PS). For  $W < W_c \sim 6.0t$ , as expected,  $r$  increases with the system size approaching the average value for the WD distribution while for  $W > W_c$ ,  $r$  decreases as the system size increases and approaches the average value for the PS. The second and third panels of Fig. 1 show the most important results of our work, namely, the ratio of the typical to the average value for the local DOS  $\rho_{typ}(\omega = 0)/\rho_{avg}(\omega = 0)$  and the scattering rate  $\Gamma_{typ}(\omega = 0)/\Gamma_{avg}(\omega = 0)$  calculated at the middle of the many-body spectrum and for  $\omega = 0$ . In the delocalized phase for very weak disorder, the typical value is of the order of the average value, both for the local DOS and the scattering rate. As the disorder strength increases, while still being less than  $W_c$ , the ratio of the typical to the average value increases with the system size approaching one. In marked contrast to this, in the MBL phase for  $W > W_c$ , the typical value of the local DOS and the scattering rate becomes much smaller than the corresponding average values such that the ratio of typical to average values for both the quantities show a clear approach to almost zero without any significant dependence on the system size.

Interestingly, the behavior of the infinite temperature typical LDOS for the MBL phase has strong similarity with the ground state LDOS of the non-interacting Anderson localized systems. In non-interacting disordered systems also the most probable value of the LDOS in the ground state is known to vanish on the localized side of the Anderson localization transition [55–57]. In the strongly localized phase of the Anderson transition, the single particle wavefunction is exponentially suppressed at sites away from the localized site and hence the probability of a particle to return to its initial position in the long time limit is finite. It was shown that the finite return probability implies a dense distribution of poles

on the real axis of the single-particle Green's function in contrast to extended states, which are given by a branch cut on the real axis of the single particle Green's function [57]. This results in vanishingly small values of the typical LDOS (of the order of broadening  $\eta$ ) in the Anderson localized phase. Here, we show a clear indication that these local observables obtained from single particle Green's functions can also be used to track the transition from a delocalized to the many-body localized phase. For this, it is necessary to focus on the higher energy states corresponding to the infinite temperature physics rather than analyzing the ground states as in the case of non-interacting Anderson localization.

It is instructive to investigate the complete probability distribution of the LDOS and the scattering rate rather than just looking at the typical and the average values. In Fig. 2 we have shown the probability distribution function of  $\rho_i = \rho_n(i, \omega = 0)$  and the scattering rate  $\Gamma_i = \Gamma_n(i, \omega = 0)$  for eigenstates  $E_n$  in the middle of the many body spectrum. For weak disorder, both the quantities have broad distributions with the arithmetic mean and the typical value being close to the most probable value of the distribution. Fits of our numerical data (shown in the figure as solid lines) reveal that the distribution functions are close to log-normal distribution for both the quantities in the delocalized phase. It is interesting to note that using the supersymmetric  $\sigma$ -model approach, quasi-one dimensional disordered metallic phase has been shown to have log-normal distribution of the LDOS in the ground state [43].

As the disorder strength increases such that  $W < W_c$ , the peak of the distribution shifts towards lower values and long tails develop. As  $W$  increases further beyond  $W_c$ , more weight gets transferred to extremely low values of both the LDOS and the scattering rates and the width of the distribution reduces significantly. Thus in the strong MBL phase the distribution is almost a delta distribution and the typical value vanishes but the arithmetic average remains finite. This trend of the probability distribution of the scattering rates is qualitatively consistent with the analysis by Basko et. al [2]. Though we have primarily focused on the zero frequency behavior of the LDOS and the scattering rates, we also investigated the finite frequency behavior of typical LDOS  $\rho_{typ}(\omega)$  and typical scattering rate  $\Gamma_{typ}(\omega)$  (shown in Fig. 2 in the Supplementary Material (SM) [58]) More or less the same features as the zero frequency case are expected to be seen in the finite  $\omega$  LDOS and self energy as well. This is clear from the fact that at all  $\omega$  within the band width, the typical value of the LDOS as well as typical value of imaginary part of the self energy decreases as the disorder strength increases.

So far we have presented details of the LDOS and the self energy, which are calculated in the middle of the many-body spectrum. In order to see whether the LDOS and the scattering rate carry signatures of transition



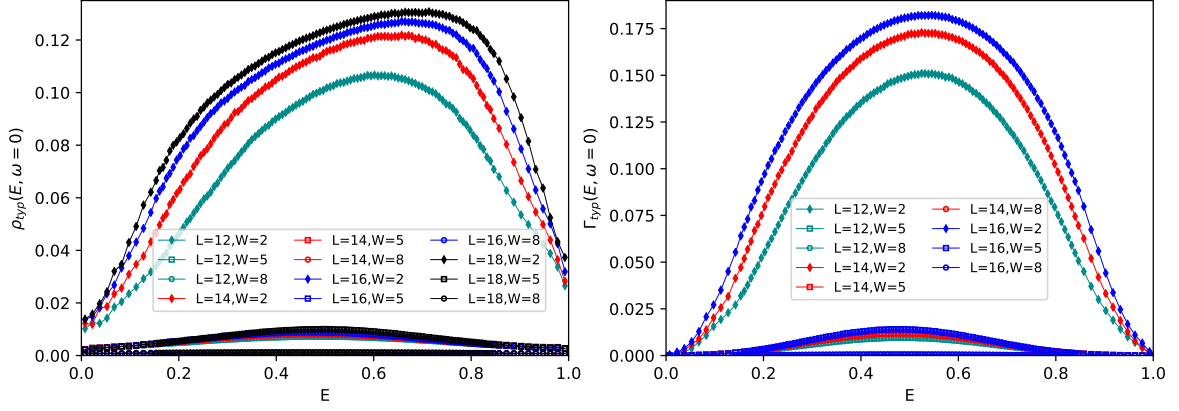


FIG. 3: The typical LDOS  $\rho_{typ}(E, \omega = 0)$  and typical scattering rate  $\Gamma_{typ}(E, \omega = 0)$  vs the rescaled eigen-energy  $E$  for three disorder strengths and various system sizes. Typical value of the scattering rate first vanishes for the eigenstates at the edges of the spectrum and a much larger disorder strength is required to make it vanishingly small for the states in the middle of the spectrum. A similar picture is depicted in the left panel which shows the typical LDOS vs  $E$ , and both of these are consistent with the energy resolved level spacing ratio shown in SM. The top most curves are for  $W = 2t$  and lower sets are higher disorder values  $5t$  and  $8t$  respectively.

across the many-body spectrum and particularly whether one can identify many-body mobility edges with these quantities, we analyzed the single particle Green's functions in the entire many-body spectrum. Fig. 3 shows the typical value of the LDOS  $\rho_{typ}(E, \omega = 0)$  vs the rescaled energy  $E$ . As the disorder strength increases, first the typical value of the LDOS at the edges of the spectrum vanishes and it requires much stronger disorder strength to make the typical DOS at the middle of the spectrum vanishingly small. For  $W > W_c$ , both the typical LDOS and the scattering rate are vanishingly small over the entire many-body eigenspectrum. This is qualitatively consistent with what is observed in the energy-resolved level spacing ratio shown in the SM [58]. A careful look at Fig. 3 shows that for the localized states the typical value of the LDOS is less than the broadening  $\eta$ . In contrast to this for the delocalized states in the middle of the spectrum the typical LDOS increases with the system size for weak disorder. In terms of the ratio of the typical to average value of the LDOS, shown in the SM [58], we see that the ratio is of the order one for states in the middle of the spectrum and decreases for states on the edges of the spectrum, giving a picture consistent with the mobility edges obtained from level spacing ratio.

Interestingly, similar features are seen in the typical value of the scattering rates obtained from the eigenstate self energy. The right panel of Fig. 3 shows  $\Gamma$  vs the eigenenergy (rescaled) for various disorder strengths. Again, we observe that the scattering rates are smaller for states at the edges of the many-body spectrum while for states in the middle of the spectrum  $\Gamma \gg \eta$  and also increases with the system size. As the disorder strength increases, first the scattering rates at the edges of the spec-

trum vanishes, and in the strongly disordered MBL phase  $\Gamma \leq \eta$  for the entire spectrum. Finally, we present results obtained by ensemble average over the entire eigenspectrum, which is equivalent to exact infinite temperature calculation. As shown in the SM [58], the behavior of the typical value of the ensemble averaged LDOS as well as the typical scattering rate is completely analogous to the corresponding mid-spectrum quantities.

In summary, we studied the single particle Green's function in the infinite temperature limit across the delocalization to MBL transition in a one-dimensional system of spin-less fermions. We demonstrated that the typical value of the infinite temperature LDOS at  $\omega = 0$  is non-zero for weak disorder in the delocalized thermal phase and it vanishes in the MBL phase. Similar features are observed in the probability distribution of the scattering rates, obtained from the imaginary part of the Dyson self energy at  $\omega = 0$ . In the delocalized phase, the scattering rate and the typical LDOS have broad log-normal distributions with a finite most probable value comparable to the arithmetic average of the distribution. In contrast in the localized phase both the scattering rate and the LDOS have a delta function like distribution peaked around zero. The MBL transition point obtained from the analysis of the typical LDOS and scattering rate is close to the one obtained from the level spacing statistics. We further propose, that many-body mobility edges can be identified from energy resolved scattering rates and the LDOS at  $\omega = 0$  obtained from the eigenstate Green's function.

An advantage of this criterion is that it provides a clear connection between the Anderson localization and the MBL. The LDOS in the infinite temperature limit for

the MBL system studied here has a similar behavior as the LDOS in the ground state of the Anderson localized system. In order to understand the origin of the behavior of the LDOS for the MBL system with the rigor with which it is known for the Anderson localized system, a perturbative analysis in the interaction strength is required, which will be done in future work. Behavior of the scattering rate can then be understood in terms of those of the LDOS using Fermi's Golden rule. Even more importantly, both these quantities can be measured in experiments directly. Given the recent developments in the field of optical lattices, it has become possible to measure single-particle spectral functions in ultracold lattices in disordered potentials [59]. We hope very much that these experiments can be extended also for the MBL systems which will shine light on the local density of states obtainable by integrating spectral functions in momentum space; and the scattering rates which determine the width of the spectral functions.

A.G. acknowledges Science and Engineering Research Board (SERB) of Department of Science and Technology (DST), India under grant No. CRG/2018/003269 for financial support. A.J. and V.R.C acknowledge funding from the Department of Atomic Energy, India under the project number 12-R&D-NIS-5.00-0100.

- 
- [1] P. W. Anderson, Phys. Rev. **109**, 1492 (1958).
  - [2] D. M. Basko, I. L. Aleiner, and B. L. Altshuler, Ann. Phys. (Amsterdam), **321**, 1126 (2006).
  - [3] E. Altman and R. Vosk, Ann. Rev. Cond. Matt. Phys. **6**, 383 (2015); E. Altman, Nature Physics, **14**, 979 (2018).
  - [4] F. Alet, and N. Laflorencie, C. R. Physique **19**, 498 (2018).
  - [5] R. Nandkishore and D. A. Huse, Ann. Rev. Cond. Mat. Phys. **6**, 15 (2015).
  - [6] D. A. Abanin, E. Altman, I. Bloch, and M. Serbyn, Rev. Mod. Phys. **91**, 021001 (2019).
  - [7] J. M. Deutsch, Phys. Rev. A **43**, 2046 (1991).
  - [8] M. Srednicki, Phys. Rev. E **50**, 888 (1994).
  - [9] M. Rigol, V. Dunjko, and M. Olshanii, Nature (London), **452**, 854 (2008).
  - [10] D. J. Luitz, N. Laflorencie, and F. Alet, Phys. Rev. B **93**, 060201(R) (2016).
  - [11] D. J. Luitz, and Y. Bar Lev, Ann. Phys. **529**, 1600350 (2017).
  - [12] E. V. H. Doggen et. al. , Phys. Rev. B **98**, 174202 (2018).
  - [13] E. V. H. Doggen and A. D. Mirlin, Phys. Rev. B **100**, 104203 (2019).
  - [14] S. Nag and A. Garg, Phys. Rev. B **99**, 224203 (2019).
  - [15] Y. Prasad and A. Garg, Phys. Rev. B **103**, 064203 (2021).
  - [16] M. Schreiber, S. S. Hodgmann, P. Bordia, H. P. Luschen, M. H. Fischer, R. Vosk, E. Altman, U. Schneider, and I. Bloch, Science **349**, 842 (2015); P. Bordia, H. P. Luschen, S. S. Hodgman, M. Schreiber, I. Bloch, and U. Schneider, Phys. Rev. Lett. **116**, 140401 (2016); H. P. Luschen, P. Bordia, S. Scherg, F. Alet, E. Altman, U. Schneider, I. Bloch, Phys. Rev. Lett. **119**, 260401 (2017).
  - [17] M. Serbyn, Z. Papic, and D. A. Abanin, Phys. Rev. Lett. **111**, 127201 (2013).
  - [18] M. Serbyn, Z. Papic, and D. A. Abanin, Phys. Rev. B **96**, 104201 (2017).
  - [19] E. J. Torres-Herrera and L. F. Santos, Ann. Phys., **1600284** (2017).
  - [20] D. J. Luitz, I. M. Khaymovich and Y. Bar Lev, SciPost Phys. Core **2**, 006 (2020).
  - [21] K. S. Tikhonov, A. D. Mirlin, and M. A. Skvortsov, Phys. Rev. B **94**, 220203(R) (2016).
  - [22] S. Iyer, V. Oganesyan, G. Refael, and D. A. Huse, Phys. Rev. B **87**, 134202 (2013).
  - [23] J. A. Kjall, H. H. Bardarson, and F. Pollmann, Phys. Rev. Lett. **113**, 107204 (2014).
  - [24] S. Bera, H. Schomerus, F. H-Meisner, and J. H. Bardarson, Phys. Rev. Lett. **115**, 046603 (2015).
  - [25] D. J. Luitz, N. Laflorencie, F. Alet, Phys. Rev. B **91**, 081103(R) (2015).
  - [26] X. Li, S. Ganeshan, J. H. Pixley, and S. D. Sarma, Phys. Rev. Lett. **115**, 186601 (2015).
  - [27] P. Naldesi, E. Ercolessi, and T. Roscilde, SciPost Phys. **1**, 010 (2016).
  - [28] S. Nag and A. Garg, Phys. Rev. B **96**, 060203(R) (2017)
  - [29] A. Samanta, K. Damle, and R. Sensarma, Phys. Rev. B **102**, 104201 (2020).
  - [30] A. De Luca and A. Scardicchio 2013 Euro. Phys. Lett. **101**, 37003 (2013).
  - [31] Leonardo Benini, Piero Naldesi, Rudolf A. Römer, Tommaso Roscilde, arXiv:2008.12719.
  - [32] R. Modak and S. Mukerjee, Phys. Rev. Lett. **115**, 230401 (2015).
  - [33] S. Mukherjee, S. Nag and A. Garg, Phys. Rev. B **97**, 144202 (2018).
  - [34] S. Bera, G. De Tomasi, F. Weiner, F. Evers, Phys. Rev. Lett. **118**, 196801 (2017).
  - [35] B. Kloss and Y. Bar Lev, Phys. Rev. B, **102**, 060201(R) (2020).
  - [36] F. Weiner, F. Evers, and S. Bera, Phys. Rev. B. **100**, 104204 (2019).
  - [37] Y. Bar Lev, D. M. Kennes, C. Klöckner, D. R. Reichman, and C. Karrasch, Euro. Phys. Lett. **119**, 37003 (2017).
  - [38] K. Agarwal, S. Gopalakrishnan, M. Knap, M. Müller, and E. Demler, Phys. Rev. Lett. **114**, 160401 (2015).
  - [39] F. Setiawan, D.L. Deng, and J. H. Pixley, Phys. Rev. B **96**, 104205 (2017).
  - [40] S. Ghosh, J. Gidugu, and S. Mukerjee, Phys. Rev. B **102**, 224203 (2020).
  - [41] Fusayoshi J. Ohkawa, J. Phys. Soc. Jpn. **52**, 1710 (1983).
  - [42] A. D. Mirlin and Y. V. Fyodorov, Phys. Rev. Lett. **72**, 526 (1994).
  - [43] A. D. Mirlin, Phys. Rev. B **53**, 1186 (1996).
  - [44] F. X. Bronold, A. Alvermann, and H. Fehske, Philos. Mag. **84**, 673 (2004).
  - [45] A. Alvermann and H. Fehske, Eur. Phys. J. B **48**, 295 (2005).
  - [46] A. Alvermann and H. Fehske, Lect. Notes Phys. **739**, 505 (2008).
  - [47] Yun Song, W. A. Atkinson, and R. Wortis, Phys. Rev. B **76**, 045105 (2007).

- [48] G. Schubert, J. Schleede, K. Byczuk, H. Fehske, and D. Vollhardt, Phys. Rev. B **81**, 155106 (2010).
- [49] *50 years of Anderson localization*, by E. Abrahams, World Scientific Publishing (2010).
- [50] M. Tarzia, Phys. Rev. B **102**, 014208 (2020)
- [51] S. Roy and D. E. Logan, Phys. Rev. Lett. **125**, 250402 (2020).
- [52] K. Byczuk, W. Hofstetter, and D. Vollhardt, Phys. Rev. Lett. **94**, 056404 (2005); E. Z. Kuchinskii, I. A. Nekrasov, M. V. Sadovski, Jour. Expt. and Theo. Phys. **106**, 581 (2008); M. C. O. Aguiar, V. Dobrosavljević, E. Abrahams, and G. Kotliar, Phys. Rev. Lett. **102**, 156402 (2009); D. Semmler, K. Byczuk, W. Hofstetter Phys. Rev. B **84**, 115113 (2011); S. Sen, H. Terletska, J. Moreno, N. S. Vidhyadhiraja, and M. Jarrell, Phys. Rev. B **94**, 235104 (2016); H. Terletska, Yi Zhang, Ka-Ming Tam, T. Berlijn, L. Chioncel, N. S. Vidhyadhiraja and M. Jarrell, Appl. Sci. **8**, 2401 (2018).
- [53] J. C. Szabo, K. Lee, V. Madhavan, and N. Trivedi, Phys. Rev. Lett. **124**, 13702 (2020).
- [54] Under Jordan-Wigner transformation, the model of spinless fermions in Eqn (1) maps onto a spin-1/2 model with spin-exchange couplings  $J_x = J_y = -2t$  and  $J_z = V$ .
- [55] D J Thouless, J. Phys. C: Solid State Phys. **3** 1559 (1970).
- [56] R Abou-Chacra, P W Anderson and D J Thouless, J. Phys. C Solid State Phys., **6**, 1734 (1973).
- [57] E. N. Economou and Morrel H. Cohen, Phys. Rev. B **5**, 2931 (1972).
- [58] See supplementary material.
- [59] V. V. Volchkov, M. Pasek, V. Denechaud, M. Mukhtar, A. Aspect, D. Delande, and V. Josse, Phys. Rev. Lett. **120**, 060404 (2018).

# Supplementary material for “Local density of states and scattering rates across the many-body localization transition”

Atanu Jana<sup>1</sup>, V. Ravi Chandra<sup>1</sup>, Arti Garg<sup>2</sup>

<sup>1</sup> *School of Physical Sciences, National Institute of Science Education  
and Research Bhubaneswar, HBNI, Jatni, Odisha 752050, India and*

<sup>2</sup> *Theory Division, Saha Institute of Nuclear Physics, 1/AF Bidhannagar, Kolkata 700 064, India*



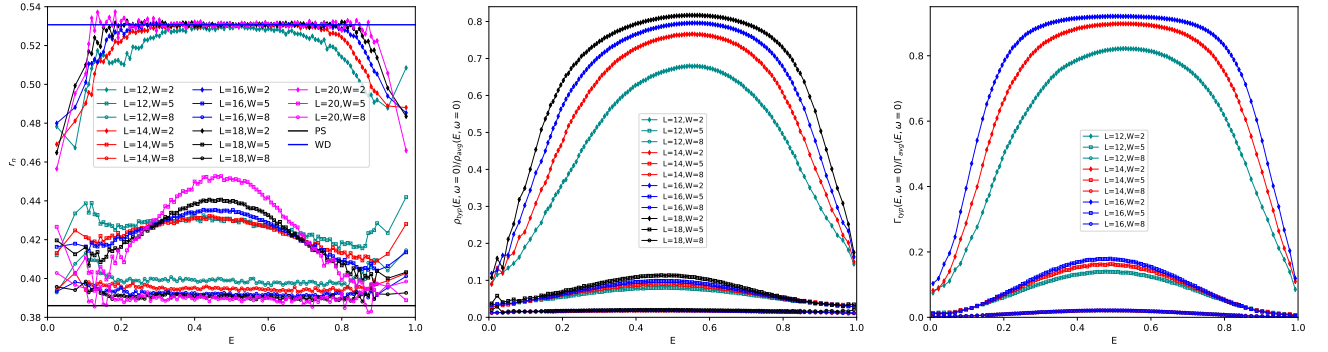


FIG. 1: First panel: The disorder averaged level spacing ratio as a function of rescaled energy  $E$  for various system sizes and disorder strengths  $W = 2, 5, 8$ . Middle panel: the ratio of the typical to average local DOS  $\rho_{typ}(\omega = 0)/\rho_{avg}(\omega = 0)$ , as a function of  $E$ . The ratio is of order one for  $W \ll W_c$  and increases with  $L$ . For  $W \gg W_c$ , the ratio is vanishingly small and does not show any clear system size dependence. Similar trend is seen in the disorder averaged ratio of typical to average value of the scattering rate  $\Gamma_{typ}(\omega = 0)/\Gamma_{avg}(\omega = 0)$ , shown in the right most panel.

### MANY BODY MOBILITY EDGES

In the main text in Fig. 3 we analyzed the behavior over the entire energy spectrum of the typical values of the LDOS and the scattering rate. We now compare the behavior of these quantities with that of the level spacing ratio as a function of energy. In Fig. 1, in the left panel we show the disorder averaged level spacing ratio as a function of rescaled energy for three different disorder strengths and different chain lengths. Because of the different statistical limits, Wigner Dyson or Poissonian, for delocalized and localized states respectively we expect a crossing point in the energy resolved level spacing plot to be an indication of a many body mobility edge for a given disorder strength. The second and third panels of Fig. 1 shows the ratio of the typical to average values of the LDOS and the scattering rates respectively. We see clearly that apart from the general trend of the ratios of these quantities becoming small as the disorder strength is increased, their values become nearly independent of the chain length in the same region of the eigenspectrum where we find localized states with Poissonian Statistics (PS) in the level spacing plot. Thus, the single particle Green's functions also provide evidence of the many body mobility edges that is consistent with the hints given by the statistics of level spacing ratios. As mentioned in the main text the level spacing ratio shown in Fig. 1 is averaged over many more disorder realizations compared to the Green's function quantities (whose computational cost is substantially more than that of the evaluation of the spectrum). However, the approximate location of the characteristic energy scale associated with the mobility edges, is consistent for all the quantities. For all our calculations the largest error in the level spacing ratios (the standard error of the mean) is of the order of  $10^{-3}$  and most ratios are substantially more accurate.

### LDOS AND SCATTERING RATES AT FINITE FREQUENCIES

We have also analyzed the eigenstate Green's functions at a finite frequency which can have a bearing for example on tunneling experiments with a finite bias voltage. Fig. 2 depicts the behavior of the finite  $\omega$  response for three different chain lengths for different disorder strengths. We choose a sufficiently large  $\omega$  range to cover all possible contributions from the Lehmann sum for  $G_n(i, j, \omega)$ . We see that for the full range of  $\omega$  chosen the  $\rho_{typ}(\omega)$  and  $\Gamma_{typ}(\omega)$  go to vanishingly small values for disorder strengths strong enough to localize the system, as in the  $\omega = 0$  case. The data in Fig. 2 has been calculated at the middle of the spectrum. Unlike in the  $\omega = 0$  case, for disorder averaging we use a single state nearest to (greater than or equal to) rescaled energy  $E = 0.5$ . Though quantitative details may vary, the general trend of the finite frequency disorder averaged  $Im[G_n(i, i, \omega)]$  and  $Im[\Sigma_n(i, i, \omega)]$  becoming vanishingly small beyond the critical disorder strength will not change if the computationally more expensive evaluation using a small energy bin as is carried out.

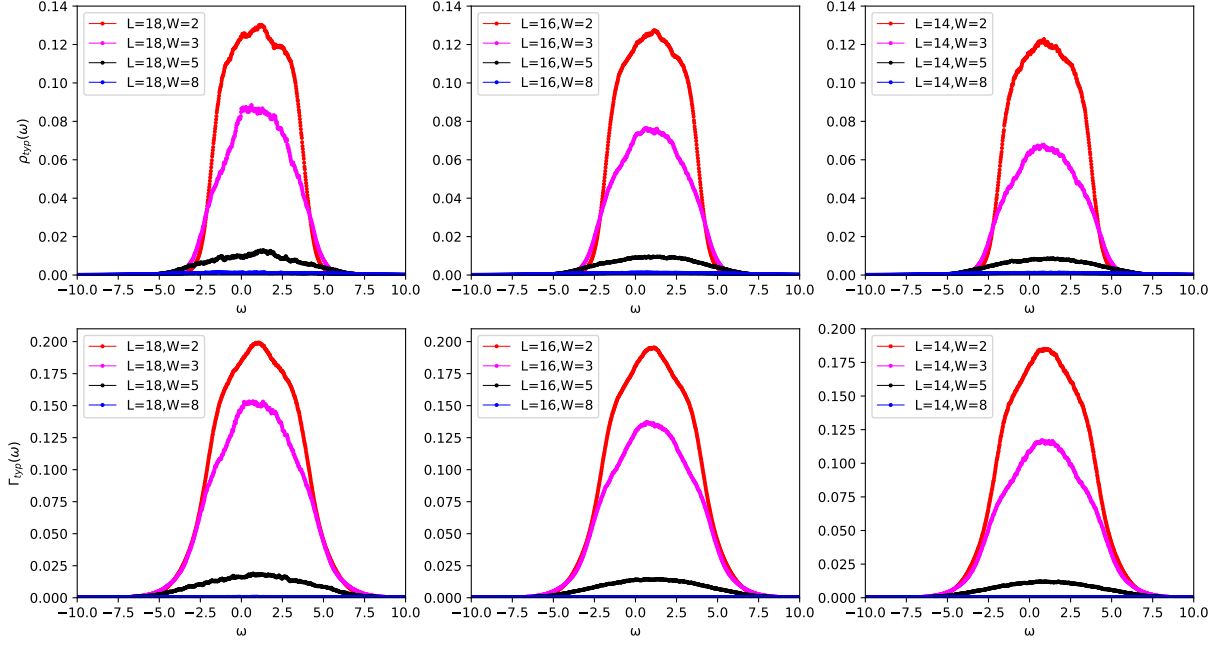


FIG. 2:  $\rho_{typ}(\omega)$  and  $\Gamma_{typ}(\omega)$  vs  $\omega$  for  $L = 14, 16, 18$  for various disorder strengths  $W = 2, 3, 5, 8$ . The data shown has been obtained using a single state nearest to the rescaled energy in the middle of the many-body spectrum, that is,  $E \approx 0.5$  for every disorder configuration.

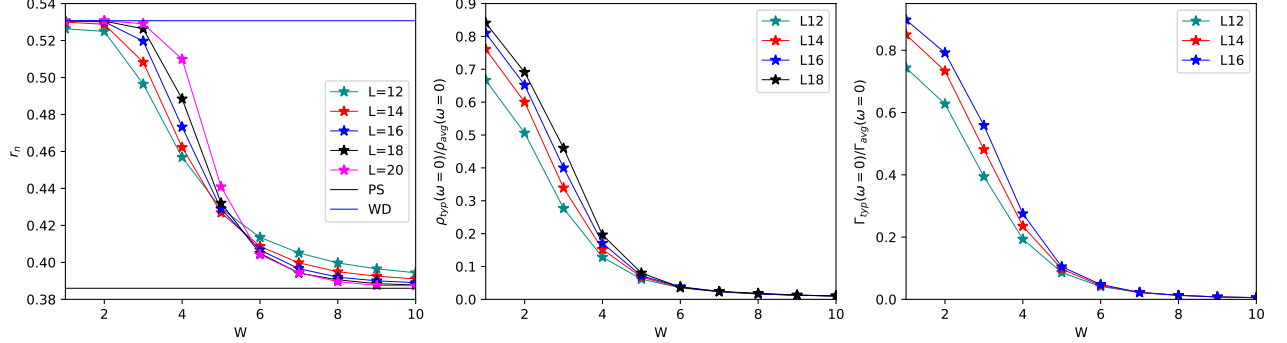


FIG. 3: First Panel: Level spacing ratio averaged over the entire spectrum vs disorder strength. Second and third panels show the ratio of typical to average values of the LDOS and scattering rates averaged over the entire spectrum vs disorder strength for various system sizes.

### INFINITE TEMPERATURE ENSEMBLE AVERAGED LDOS AND SCATTERING RATES

In the main text in Fig.1 we have presented the the ratio of the typical to average LDOS and scattering rate, calculated for the mid spectrum eigenstates at  $\omega = 0$ , as a function of the disorder strength. Here we have shown results obtained by ensemble average over the entire eigenspectrum in the infinite temperature limit. As shown in Fig. 3, the behavior of the LDOS and the scattering rates calculated from infinite temperature ensemble average is qualitatively consistent with that obtained from the analysis of mid spectra Green's function. The typical value of the LDOS as well as the typical scattering rate decreases as the disorder strength increases becoming vanishingly small for  $W > W_c$  having no significant system size dependence. For comparison we have shown level spacing ratio averaged over the entire spectrum in the first panel of Fig. 3.